ISSN: 2096-3246
Volume 58, Issue 01, 2026

MVIT: A NOVEL TRANSFORMER-BASED APPROACH FOR COLON CANCER CLASSIFICATION USING HISTOPATHOLOGICAL IMAGES

[1]Himanshu Vishwakarma, [2]Prem Chand Yadava, [3]Ajay Kumar Maurya , [4]Nimisha Yadav, [5]Vishal Yadav and [6]Ravi Prakash

[1, 2,3,5,6] Department of Electronics Engineering, Uma Nath Singh Institute of Engineering and Technology, Veer
Bahadur Singh Purvanchal University Jaunpur, Uttar Pradesh-222003
[4]Department of Mathematics, Uma Nath Singh Institute of Engineering and Technology, Veer Bahadur
Singh Purvanchal University Jaunpur, Uttar Pradesh-222003
Email Id: [1]hvhim07@gmail.com, [2]pcyadavknit@gmail.com, [3]ajaybtech84@gmail.com,
[4]nimishavbspu@gmail.com, [5]vishalunsiet@gmail.com, [6]ravirim75@gmail.com

Abstract: Colon cancer must be accurately and promptly detected in order to improve patient outcomes and direct the development of effective treatment plans. In this paper, a unique Modified Vision Transformer (MViT) architecture designed for automated colon histopathology image classification into benign and cancer categories is presented. The MViT efficiently extracts global contextual information from intricate tissue structures by incorporating unique improvements into the conventional transformer design A publicly accessible dataset was used to train and evaluate the model, which produced an astounding 99.3% classification accuracy. It continuously outperformed a number of leading-edge deep learning and hybrid models in important assessment measures, such as ROC-AUC (0.99), precision (0.9940), recall (0.9920), and F1-score (0.9930). These outcomes highlight the model's strong discriminative power and dependability. All things considered, the suggested MViT framework offers a strong and effective method for analysing histopathological images and has a great chance of being integrated into computer-aided diagnostic (CAD) systems to improve clinical judgment when diagnosing colon cancer.

Keywords: Classification, Modified Vision Transformer (MViT) model, deep learning, Histopathological images

1.Introduction: Around the world, colon cancer affects both men and women and is a cancer that is commonly diagnosed. Environmental exposures and genetic predisposition work together to influence its development [1]. People over 50 are far more likely to get colon cancer, and those with a family history of the disease are at a much higher risk [2]. Its start and progression are also influenced by a number of lifestyle factors [3]. These include smoking, drinking alcohol, eating too much red meat, and being obese all of which have been closely linked to an increased risk of colon cancer. Regular screening is an important preventive intervention since early diagnosis is essential for improving treatment results and patient survival rates [4Adenocarcinomas account for around 90% of colon malignancies, with spindle cell, squamous, and undifferentiated carcinomas being less frequent histological variations [5,6]. Early detection of colon cancer reduces the duration of therapy, improves treatment precision, and dramatically lowers death rates [7, 8]. For early diagnosis, routine screening is

essential, especially for asymptomatic people, those receiving therapy, and those under post-treatment surveillance. However, healthcare systems are under a lot of strain due to the growing need for regular tests, which raises operational costs and clinician workload [9]. Computer-aided diagnostic (CAD) systems are being incorporated into clinical practice to help address these issues. Conventional analytical techniques are becoming more and more insufficient for efficiently processing and understanding large-scale datasets as medical data continues to expand exponentially [11].In contrast, deep learning methods offer a powerful alternative by automatically learning relevant features from complex datasets without manual intervention. Once trained, such models are evaluated using standard performance metrics to validate their effectiveness [12 In this paper, a new framework for colon cancer classification through MViT is introduced. Therefore, we require a new effective model in a compacted version which can carry out the same tasks but with fewer computational burdens. We are basically aiming at applying the vision transformer (ViT) architecture for the classification of colon cancer through histopathology images. Some of the contributions made by our proposed approach have been stated below. In order to restore edges and keep all details intact, ant colony optimization-based reformed fourth-order partial differential equation has been applied. ViT model was successfully applied in colon cancer classification .Positional embedding is used sequentially on the image patches to retain the positional information. A distinct set of demonstrations is added at the beginning to place the embedded patches in the correct position. A comprehensive analysis is done by varying the size of the patches and observing the result. It is observed that the model provides the best accuracy when the size of the patches is 16 x 16.A fine-tuning strategy is used to vary the values of hyperparameters to increase the accuracy and normalize the model. A novel MViT is proposed for the colon cancer abnormalities classification in a single framework using histopathological images. The rest of this paper is organized as follows: The second section describes some existing approaches. The third section explains the methodology and materials. This includes a discussion of the data sets used and a brief explanation of the approach used in this work. The fourth section describes the performance measures employed. The fifth section discuss the proposed approach qualitatively and quantitatively. The sixth section explains the results of the proposed approach. Finally, Section seventh section concludes the paper.

2.Related Work: Extensive research has been conducted on cancer diagnosis using machine learning (ML) and deep learning (DL) techniques, particularly in histopathological image classification. Sirinukunwattana et al. proposed a method combining SoftMax CNN with NEP, achieving an F1-score of 0.784 and a multiclass AUC of 0.917, outperforming other contemporary techniques. Their approach demonstrated promise for quantitative tissue analysis in pathology and contributed to a deeper understanding of cancer development [13] Godkhindi et al. employed machine learning algorithms for cancer classification, reporting accuracies of 85% (Random Forest), 87% (CNN), and 83% (KNN), thus showing the superior performance of DL over traditional ML methods [14]. Wang et al. developed a DL-based approach to predict Tumour Mutation Burden (TMB) using H&E-stained histopathological images. Their model achieved an AUC exceeding 0.75 and an accuracy of 82% using VGG19, validating its clinical relevance [15]. Similarly, Vuong et al. utilized DenseNet121 to classify tumour tissues into four

categories, attaining an accuracy of 85.91% and demonstrating the effectiveness of deep models for full-slide image analysis [16]. Sitnik et al. found minor differences between training classifiers from scratch and using pre-trained models; their U Net++ model achieved a micro-balanced accuracy of 89.34%, with an F1-score of 83.67% [17]. In the case of colon histology, Ribeiro et al. have shown that CNN outperforms the conventional hand-crafted feature extraction methods for classification of colon mucosa with an accuracy of 90.96% [18]. In the case of colon histology, Ribeiro et al. have shown that CNN outperforms the conventional hand-crafted feature extraction methods for classification of colon mucosa with an accuracy of 90.96% [18].Yildirim et al. designed a CNN called MA Colon NET that provided an astounding accuracy of 99.75%, proving its effectiveness for detecting colon cancers [19]. Another work by Kumar et al. on the design of CRCCN-Net is a lightweight CNN that has an accuracy of 99.21%, precision of 99.18% and F1-score of 0.9870 [2] The notion of CAD was first coined by Lee Lusted in 1955, while early studies such as Lodwick's study on digitizing chest radiography in 1963 paved the path towards computer-aided diagnostics [21, 22]. The idea of computer-aided diagnosis is increasingly becoming a very popular topic of research in the domain of medical imaging. There has been the successful application of many deep learning models to the detection of cancer diseases. For instance, Shi et al. successfully applied the multi-modal thin illustration approach to needle biopsy images, with accuracy being reported at 88.10% [24]. Another successful implementation was that of Kuruvilla and Gunavathi, who used artificial neural networks for classifying computed tomography images using the approach of numerical topography. In addition, an effective artificial neural network based on the outcome of the skewness method has proven to be very effective in the classification of the computed tomography images [25]. The authors of another study developed a non-invasive diagnostic system based on positron emission tomography images and fluorodeoxyglucose. The diagnostic technique was found to be highly effective in detecting lung cancer in the dataset that had 8,511 images [26]. Also, the success achieved in the study by Shen et al., where Multi-Crop CNN was implemented, made the technique highly efficient in detecting lung cancer, with the accuracy being reported at 87.14% [27]. Moreover, there is the study carried out by Selvanambi et al. on CNN, ResNet50, and transfer learning models like MobileNet, InceptionV3, and Xception [31, 32]. Recent research works have advanced lung cancer detection through other CNN model architecture methods [33-37]. Another author who contributed to the literature on lung cancer detection is Su et al. and came up with a modification of the Faster R-CNN (FRCNN) that was used to classify images from CTs. However, the performance of the system was quite low since there was no preprocessing stage included in the proposed method[38]. Moreover, the approach developed by Talib et al. comprised of a two-step method whereby first a transformer segmentation network was applied followed by the CNN custom network. This approach was, however, limited due to certain aspects since it involved two steps.[39]. Furthermore, Mercaldo et al. came up with an evaluation method based on different deep learning techniques such as MobileNet, VGG16/19, and AlexNet in histopathology image classification. [40] Further, Mercaldo et al. suggested an evaluation method where different architectures such as MobileNet, VGG16/19, and AlexNet were used in histopathology image classification. [40]. Although there have been several improvements, the existing methods as well as the one suggested by other researchers have had challenges

concerning the preprocessing stage as there have been challenges with regard to denoising, enhancing and preserving edges. Moreover, the challenge has been in trying to ensure that the methods of classification achieve accurate results in detecting the relevant abnormalities. There has been sensitivity problems with regard to the use of these architectures, mainly due to poor performance regarding noise and quality issues.

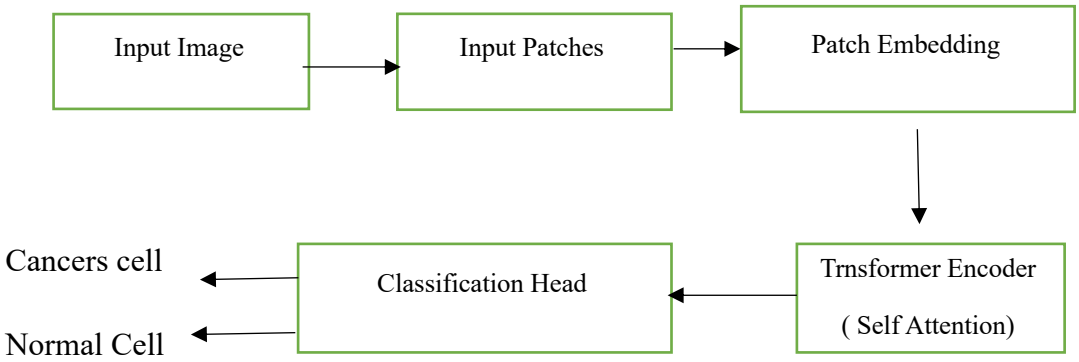

Fig1 : Block Diagram of proposed Modified Vision Transformer for colon cancer classification

3.Method and Models : The proposed method for cancer classification using histopathological image analysis is based on the following image classification pipeline, which is based on advanced image preprocessing and the application of deep learning techniques. The first stage in the image classification pipeline is the application of the ACO-RFPDE algorithm, which is an advanced image preprocessing technique that combines the Ant Colony Optimization (ACO) and Reformed Fourth-Order Partial Differential Equation (RFPDE) techniques. The application of this algorithm is essential in the image classification pipeline, as it enhances the quality of the image, thus improving the edges, which are important in the image feature extraction stage. In order to ensure the thoroughness and objectivity of the image classification model, the image dataset is split into the training set (80%), the validation set (10%), and the test set (10%) after the image enhancement stage. The VGG Image Annotator (VIA) is the image annotation tool that is applied in the image classification pipeline. The image annotation is important, as the model needs to learn and identify the relevant patterns and morphological structures in the histopathological tissue images. The Modified Vision Transformer (MViT) is the advanced image classification model that is based on the Vision Transformer (ViT) model, which is specially designed for medical image processing. In order to effectively address such intricate and fine-grained features, which are common in histopathology data, these changes are most likely related to improvements in attention mechanisms or architectures. The MViT model has been trained on these datasets, and its goal is to classify images into two classes: Colon Benign and Colon Adenocarcinoma . Once the training process has been successfully completed, the performance of the model has been assessed using critical classification metrics such as Accuracy, True Positive Rate (TPR), True Negative Rate (TNR), Precision, and F1-score. This

gives a complete idea of how effectively the model has been able to classify and distinguish between benign and malignant samples of colon tissue types. It has to be noted here that, although the title of this figure suggests a classification problem related to colon cancer, the actual classes are related to colon tissue types, and this has to be corrected in future versions. To summarize, the proposed pipeline has effectively used cutting-edge preprocessing and deep learning techniques to improve the precision and accuracy of cancer classification in images.

The proposed model uses a Modified Vision Transformer (ViT) architecture to classify colon cancer images accurately from the biopsy images. The overall process of the model can be represented as shown in Fig. 2 . First of all, the input colon biopsy image is divided into patches and then these patches are embedded using the patch embedding process. After the embedding of the patches, the transformer network is used to extract the features of the images.$\boldsymbol{I} \in \mathbb{R}^{\boldsymbol{H}\times\boldsymbol{W}\times\boldsymbol{C}}$is divided into non-overlapping patches of size $\boldsymbol{P}\times\boldsymbol{P}$. The total number of patches is given by $\boldsymbol{N}=\frac{\boldsymbol{HW}}{\boldsymbol{P^2}}$. Each patch is then flattened and linearly projected into the D-dimensional embedding space, creating a sequence of patch embeddings. To include spatial information, the positional encodings are added to the patch embeddings. The output is then passed through a stack of transformer encoder layers. Each encoder consists of a multi-head self-attention mechanism (MHSA) followed by a feed-forward network (FFN), along with residual connections and layer normalization.

The self-attention mechanism computes the relationships between patches using query, key, and value matrices:

$$\text{Attention}(\boldsymbol{Q},\boldsymbol{K},\boldsymbol{V}) = \text{Softmax}\left(\frac{\boldsymbol{QK^T}}{\sqrt{\boldsymbol{d}}}\right)\boldsymbol{V}$$

This helps the model to capture global contextual dependencies, which is very important in identifying complex tissue patterns in colon cancer images. The multi-head attention mechanism helps to enhance the representation learning by looking at the information from multiple sub-spaces. The FFN further refines the features. The enhancements are made to the model to make it more robust to noise and capture the fine details of the structural components in the biopsy images. The model is now better at distinguishing between normal and cancerous tissues. The representation is then fed into the classification head, usually a fully connected layer with a softmax function, to classify the input image and find the class label.

Q (Query Matrix) , K (Key Matrix) ,V (Value Matrix) , N – Number of patches ,d – embedding dimension

3.1 Dataset : The open-source image database LC25000 is a histopathology image database for cancer classification consisting of 25,000 images of 768 x 768 pixels size. The database consists of equal numbers of images in each class, totaling to 5,000 per class. There are five different image classes in the dataset, which are colon adenocarcinoma, benign colon tissue, lung adenocarcinoma, lung squamous cell carcinoma, and benign lung tissue. This image database can be used in feature extraction and developing computer-aided diagnosis using deep learning models, as the database consists of a fairly balanced set of both malignant and non-malignant images.

Table 1: Key details of the micro biopsy lung cancer database**.**

Characteristics	Database		
Name	LC25000		
Accessibility	Openly		
Quantity of imageries	25000		
Classes	**5**	(i) Adenocarcinomas Colon	**5000**
		(ii) Benign Colon	**5000**
		(iii) Adenocarcinomas Lung	**5000**
		(iv) Squamous Cell Carcinomas Lung	**5000**
		(v) Lung Benign	**5000**
Imagery size	$\mathbf{768 \times 768}$ pixels		
Imagery format	JPEG		

3.2:Proposed Modified Vision Transformer for Classification of Colon Cancer histopathological Images:

The microscopic lung images are also accountable to photon noise. This phenomenon takings place remaining to the random spreading of particles during the achievement of images. The dispersed particles follow a path corresponding to a Poisson distribution [42]. According to literature, the distribution is naturally multiplicative, and this affects the readability of the features in the imagery.

The comprehensive explanation of the found lung microscope images [43] can be expressed as follows:

$$\boldsymbol{l_o} = \boldsymbol{l} * \boldsymbol{Poisson} \quad (\mathbf{1})$$

here $\boldsymbol{l}$ is the real lung biopsies images which is partial via the Poisson noise $\boldsymbol{\eta_2}$; $\boldsymbol{l_o}$ is the produced noisy images; and $\boldsymbol{\eta_1}$ is the additive noise. To improve the clarity of lung images and reduce noise, the technique described by Yadava et al. [44] has been utilized. This approach employs ant colony optimization and utilizes a modified fourth-order partial differential equation (ACO-RFPDE) to eliminate Poisson noise. The mathematical formulation of RFPDE is represented by:

$$\boldsymbol{l_{RFPDE}^{n+1}} = \boldsymbol{l_{ij}^{n}} + \Delta \mathbf{t}.\left[\frac{\mathbf{1}}{\boldsymbol{\lambda}} + \boldsymbol{\nabla^2}.\left(\boldsymbol{c_{MAD}}\left(\left\|\boldsymbol{\nabla^2 l_{ij}^{n}}\right\|\right)\boldsymbol{\nabla^2 i l_{ij}^{n}}\right)\right] \quad (\mathbf{2})$$

here, $\Delta \boldsymbol{t}$, $\boldsymbol{n}$ and $\boldsymbol{\lambda}$ are time constant, iterations and regularization hyperparameter which is tuned by ACO.

Later, let $\boldsymbol{D}$ offerings the denoised lung biopsy imageries dataset with total $\boldsymbol{l_N}$ images. The dataset is prepared by engaging ACO-RFPDE. Moreover, it has been divided into training, validation, and test images at a portion of 80:10:10, respectively.

For classification tasks , the total loss function can be defined as:

$$\boldsymbol{L_{total} = L_{classification} + \lambda L_{regularization}} \quad (3)$$

Where $\boldsymbol{L_{classification}}$ represents the cross- entropy loss with label smoothing

$\boldsymbol{L_{regularization}}$ introduces weight decay ($\boldsymbol{L_2 regularization}$) to mitigate overfitting

$\boldsymbol{\lambda}$ is hyperparameter controlling the impact of regularization

In improve classification loss apply label smoothing to the cross – entropy loss we get

$$\boldsymbol{L_{classification}} = -\frac{1}{N}\sum_{i=1}^{N} \sum_{c=1}^{C} \left[y_{i,c}(1-\epsilon) + \frac{\epsilon}{C}\right] log\left(y^{\wedge}_{i,c}\right) \quad (4)$$

Where

- N is the number of samples in a batch
- C is the total number of classes
- $\boldsymbol{y_{i,c}}$ denotes the one – hot encoded label for the $\boldsymbol{i^{th}}$ sample and the $\boldsymbol{c^{th}}$ class
- $\boldsymbol{y^{\wedge}_{i,c}}$ is the predicted probability for the $\boldsymbol{i^{th}}$ sample and the $\boldsymbol{c^{th}}$ class , typically obtained via a SoftMax function
- $\boldsymbol{\epsilon}$ is the label smoothing factor ($\boldsymbol{0 \leq \epsilon \geq 1}$)

To reduce overfitting , weight decay penalizes large model parameters:

$$\boldsymbol{L_{regularization}} = \sum_{w \epsilon \theta} \boldsymbol{w^2} \quad (5)$$

Where $\boldsymbol{\theta}$ is the set of trainable parameters (e.g, weights of the transformer model)

Substitute the value of equation (2) and equation (3) in equation (1) we get final loss function is

$$\boldsymbol{L_{total}} = -\frac{1}{N}\sum_{i=1}^{N} \sum_{c=1}^{C} \left[y_{i,c}(1-\epsilon) + \frac{\epsilon}{C}\right] log\left(y^{\wedge}_{i,c}\right) + \sum_{w \epsilon \theta} \boldsymbol{w^2} \quad (6)$$

Level smoothing factor ($\boldsymbol{\epsilon}$) typically set to 0.1

Regularization weight ($\boldsymbol{\lambda}$) : Commonly $\boldsymbol{10^{-4}}$ for most datasets, but this is adjustable depending on the validation performance. The study introduces a modified Vision Transformer for the classification of colon cancer in images. Due to the inclusion of Poisson noise in microscopic images, a pre-processing step is included to effectively remove noise using Ant Colony Optimization (ACO) and the Reformed Fourth-Order Partial Differential Equation (RFPDE) techniques. The clean images are used to train and evaluate the model, with an 80:10:10 split. For the classification, the study introduces an effective loss function, which is a combination of label smoothing with cross-entropy loss and weight decay with regularization. This helps to prevent overfitting and overconfidence in the model. The final loss function is an improvement on the Vision Transformer loss function to better classify cancerous and non-cancerous tissues.

4.Result and Evaluations : The projected MViT has been established and estimated with the assistance of the LC25000 [41] lung colon histopathology images dataset. This segment describes the presentation measures and experimental outline used for emerging the suggested method. In accumulation, this segment affords a numerical assessment of the anticipated MViT. The estimations have been provided in the form of relative examination for validating the suggested method.

4.1 Performance Metrics:

A table of the evaluation criteria used in the current investigation is presented in Table 2. The parameters were extracted from the classification [45] and detection [46] criteria. Specifically, there are nine evaluation metrics used in the experiment, with seven of them assessing classification criteria while two of them measuring the effectiveness of anomaly detection. All the classification criteria are calculated based on the confusion matrix. This matrix consists of four basic elements including TP, FP, FN, and TN.

Metrics	Mathematical Formula
Accuracy (ACC)	$\boldsymbol{ACC = \frac{TP+TN}{TP+TN+FP+FN}}$
True positive rate (TPR)	$\boldsymbol{TPR = \frac{TP}{TP+FN}}$
True negative rate (TNR)	$\boldsymbol{TNR = \frac{TN}{TN+FP}}$
Precision (PRC)	$\boldsymbol{PRC = \frac{TP}{TP+FP}}$
F-Score (FSC)	$\boldsymbol{FSC = \frac{2 * PC * TPR}{PC+TPR}}$
Balanced Classification Rate (BCR)	$\boldsymbol{BCR = \frac{1}{2}[TPR+TNR]}$
Youden's Index (YDI)	$\boldsymbol{YDI = TPR - (1 - TNR)}$
Dice Coefficient (DCF)	$\boldsymbol{DCF = \frac{2\lvert p \cap p^{*}\rvert}{\lvert p\rvert + \lvert p^{*}\rvert'}}$
Jaccard Index (JAC)	$\boldsymbol{JAC = \frac{\lvert p \cap p^{*}\rvert}{\lvert p \cup p^{*}\rvert'}}$
	here, $\boldsymbol{t}$ and $\boldsymbol{t^{*}}$ are the predicted bounding box and ground-truth coordinates.

5. Quantitative Analysis :

Table 3. Comparison of results with state-of-arts

Reference	Image Type	Classifier	Accuracy
[47]	Histopathological	CNN	97.2

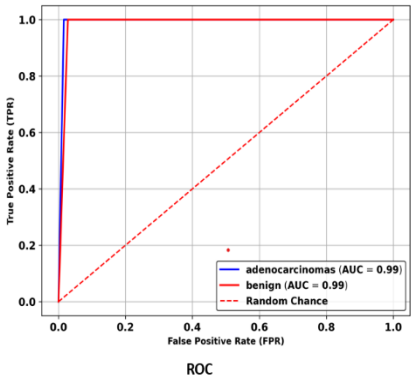

ROC

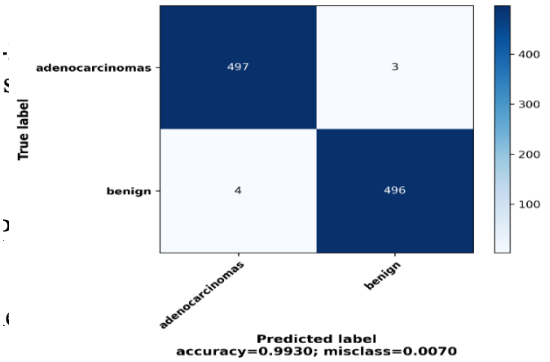

ı Transformer 98.84

Histopathological

Proposed Modified Vision 99.3

Histopathological Transformer

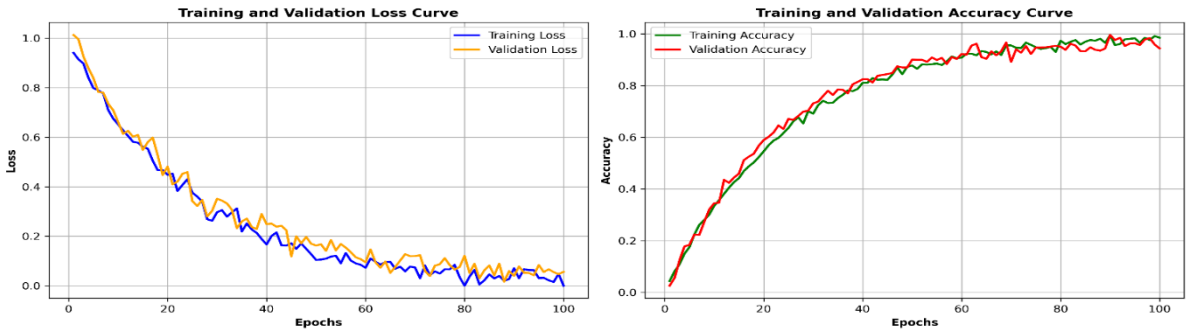

Fig.**2**(a) Training and validation loss and accuracy curve showing steady convergence and low overfitting across 100 epochs .

Fig3. Receiver Operating Characteristic (ROC) curves for both adenocarcinoma and benign classes.

Fig.4 Confusion matrix and classification metrics for the Proposed modified vision transformer model.

6. Results and Discussion: The performance of the suggested MViT model was thoroughly evaluated using the benchmark dataset that includes histopathological images segmented into adenocarcinoma and benign categories. The results achieved in this work indicate the efficacy of the MViT model for the histopathological image classification problem compared to other state-of-the-art models. As demonstrated in Table.3, a comparative analysis of the existing state-of-the-art models utilized in the cancer detection problem was carried out in this work. The state-of-the-art models included CNN, MC-CNN, ANN, ResNet50-SVM, and AlexNet-DWT-SVM. The highest accuracy achieved by the existing state-of-the-art models was 99.1% for the AlexNet-DWT-SVM model. In contrast, an accuracy of 99.3% was achieved using the MViT model and created a new benchmark in the problem area. Figures 2(a-b) show the loss and accuracy curves obtained in this study. Loss curves generated in this study consistently depict a reduction in the loss through the 100 epochs. The accuracy curves generated in this study depict the consistency of the model during training and the validation process. In this case, the proposed MViT model achieved an accuracy of 99% in the validation phase. Figure.4 presents the confusion matrix generated in this study. The proposed MViT model classified 993 images out of the total

1000 images correctly. However, only 7 images were classified wrongly by the proposed MViT model. In this regard, the model classified 497 adenocarcinoma samples and 496 benign samples resulting in an accuracy rate of 99.3%. Additional metrics have been used in evaluating the robustness of the classifier as follows; precision: 0.9940, recall (sensitivity): 0.9920, specificity: 0.9940, f1 score: 0.9930, MCC: 0.9860, Youden index: 0.9860. This implies that the MViT model maintains a good balance between the sensitivity and specificity and therefore can be effectively used in practical applications. Figure 3 presents the ROC curve for both classes. As depicted in figure 4, the area under the curve (AUC) for both classes is 0.99 which implies that the model has exceptional discriminative capabilities. It is also proved by the closeness of the ROC curve to the upper left point of the graph. It indicates the efficiency of the model in discriminating between cancer and healthy histopathological images. According to the data obtained, the efficiency of the model seems to be very high in the area of medical image recognition. It can be proved by the outstanding convergence of the model, its low rate of misclassification, and its high efficiency in different parameters. It indicates the efficiency of the model compared to other models.

7. Conclusion: The Modified Vision Transformer (MViT) model has been developed in this study to classify colon cancer images. In this regard, the proposed method succeeded in applying the transformer architecture attention mechanism to enhance the features extracted from the medical images. More importantly, the proposed model surpassed other models and achieved higher accuracy at 99.3%, and demonstrated superior performance in terms of generalization when applied to the benign and adenocarcinoma classes. In addition, the proposed model performed better compared to other models due to its robustness, which can be attributed to the high value of the MCC score and Youden index. With the promising results obtained from the experiment, the proposed model showed great potential in assisting pathologists in the decision-making process.

REFERENCES :

1. Murphy N, Ward HA, Jenab M, et al. Heterogeneity of colorectal cancer risk factors by anatomical subsite in 10 European countries: a multinational cohort study. Clin Gastroenterol Hepatol. 2019;17(7):1323-1331. https://doi.org/10.1016/j.cgh. 2018.07.030
2. Kasi PM, Shahjehan F, Cochuyt JJ, Li Z, Colibaseanu DT, Merchea A. Rising proportion of young individuals with rectal and colon cancer. Clin Colorectal Cancer. 2019;18(1):e87-e95. https://doi.org/10.1016/j.clcc.2018.10.002
3. Hassanpour SH, Dehghani M. Review of cancer from perspective of molecular. J Cancer Res Pract. 2017;4(4):127-129. https://doi.org/10.1016/j.jcrpr.2017.07.001
4. Koi M, Okita Y, Takeda K, et al. Co-morbid risk factors and NSAID use among white and black Americans that predicts overall survival from diagnosed colon cancer. PLoS One. 2020;15(10):e0239676. https://doi.org/10.1371/journal.pone. 0239676
5. Van Pelt GW, Kjær-Frifeldt S, van Krieken JHJM, et al. Scoring the tumor-stroma ratio in colon cancer: procedure and recommendations. Virchows Arch. 2018;473(4):405-412. https://doi. org/10.1007/s00428-018 2408-z
6. Bellen C, Ceuterick M, Dolimont A, Peny MO. Collision tumor: a colonic adenocarcinoma and a gastric adenocarcinoma. Acta Chir Belg. 2021;1-12. https://doi.org/10.1080/00015458.2021. 1881331
7. Banerjee A, Pathak S, Subramanium VD, Dharanivasan G, Murugesan R, Verma RS. Strategies for targeted drug delivery in treatment of colon cancer: current trends and future perspectives. Drug Discov Today. 2017;22(8):1224-1232. https://doi. org/10.1016/j.drudis.2017.05.006

8. Wang L, Duan W, Yan S, Xie Y, Wang C. Circulating long noncoding RNA colon cancer-associated transcript 2 protected by exosome as a potential biomarker for colorectal cancer. Biomed Pharmacother. 2019;113:108758. https://doi.org/10.1016/j. biopha.2019.108758
9. Jiang B, Linden PA, Gupta A, et al. Conventional computed tomographic calcium scoring vs full chest CTCS for lung cancer screening: a cost-effectiveness analysis. BMC Pulm Med. 2020; 20(1):1-7. https://doi.org/10.1186/s12890-020-01221-8
10. Yildirim M, Cinar A. A deep learning based hybrid approach for COVID-19 disease detections. Traitement du Signal. 2020;37 (3):461-468. https://doi.org/10.18280/ts.370313
11. Jan B, Farman H, Khan M, et al. Deep learning in big data analytics: a comparative study. Comput Electr Eng. 2019;75:275- 287 https://doi.org/10.1016/j.compeleceng.2017.12.009.
12. Çinar A, Yıldırım M. Detection of tumors on brain MRI images using the hybrid convolutional neural network architecture. Med Hypotheses. 2020;139:109684. https://doi.org/10.1016/j.mehy.2020.109684
13. Sirinukunwattana K, Raza SEA, Tsang YW, Snead DR, Cree IA, Rajpoot NM. Locality sensitive deep learning for detection and classification of nuclei in routine colon cancer histology images. IEEE Trans Med Imaging. 2016;35(5):1196-1206.
14. Godkhindi AM, Gowda RM. Automated detection of polyps in CT colonography images using deep learning algorithms in colon cancer diagnosis. Paper presented at: 2017 International Conference on Energy, Communication, Data Analytics and Soft Computing (ICECDS), pp. 1722–1728. IEEE; 2017.
15. Wang L, Jiao Y, Qiao Y, Zeng N, Yu R. A novel approach combined transfer learning and deep learning to predict TMB from histology image. Pattern Recog Lett. 2020;135:244-248.
16. Vuong TLT, Lee D, Kwak JT, Kim K. Multi-task deep learning for colon cancer grading. Paper presented at: 2020 International Conference on Electronics, Information, and Communication (ICEIC), pp. 1–2. IEEE; 2020.
17. Sitnik D, Aralica G, Hadžija M, et al. A dataset and a methodology for intraoperative computer-aide,diagnosis of a metastatic colon cancer in a liver. Biomed Signal Process Control. 2021;66: 102402.
18. Ribeiro E, Uhl A, Häfner M. Colonic polyp classification with convolutional neural networks. Paper presented at: 2016 IEEE 29th International Symposium on Computer-Based Medical systems (CBMS), pp. 253–258. IEEE; 2016.
19. Kumar A, Vishwakarma A, Bajaj V. Crccn-net: Automated framework for classification of colorectal tissue using histopathological images. Biomedical Signal Processing and Control. 2023 Jan 1;79:104172.
20. Yildirim M, Cinar A. Classification with respect to colon adenocarcinoma and colon benign tissue of colon histopathological images with a new CNN model: MA_ColonNET. International Journal of Imaging Systems and Technology. 2022 Jan;32(1):155-62.
21. L.B. Lusted, Medical electronics, N. Engl. J. Med. 252 (1955), 580–585.
22. G.S. Lodwick, T.E. Keats and J.P. Dorst, The coding of roentgen images for computer analysis as applied to lung cancer, Radiology 81 (1963), 185–200.
23. R. Thawani, M. McLane, N. Beig, et al., Radiomics, and radiogenomics in lung cancer: A review for the clinician,Lung Cancer 115 (2018), 34–41.
24. Y. Xu, L. Jiao, S. Wang, et al., Multi-label classification for colon cancer using histopathological images, Microsc.Res. Tech. 76 (2013), 1266–1277.

25. J. Kuruvilla and K. Gunavathi, Lung cancer classification using neural networks for CT images, Comput. MethodsPrograms Biomed. 113 (2014), 202–209.
26. S.A. Deppen, J.D. Blume, C.D.Kensinger, et al., Accuracy of FDG-PET to diagnose lung cancer in areas with infectious lung disease: A meta-analysis, JAMA J. Am. Med. Assoc. 312 (2014), 1227–1236.
27. W. Shen, M. Zhou, F. Yang, et al., Multi-crop Convolutional Neural Networks for lung nodule malignancy suspiciousness classification, Pattern Recognit. 61 (2017), 663–673.
28. W. Sun, B. Zheng andW. Qian, Automatic feature learning using multichannel ROI based on deep structured algorithms for computerized lung cancer diagnosis, Comput. Biol. Med. 89 (2017), 530–539.
29. Z. Yuan, M. Izady Yazdanabadi, D. Mokkapati, et al., Automatic polyp detection in colonoscopy videos, Med. Imaging 2017 Image Process. (2017), 101332K.
30. R. Selvanambi, J. Natarajan, M. Karuppiah, et al., Lung cancer prediction using higher-order recurrent neural network based on glowworm swarm optimization, Neural Comput. Appl. 32 (2020), 4373–4386.
31. A.O. de Carvalho Filho, A.C. Silva, A.C. de Paiva, et al., Classification of patterns of benignity and malignancy based on CT using topology-based phylogenetic diversity index and convolutional neural network, Pattern Recognit. 81 (2018), 200–212.
32. R.V.M. da N´obrega, P.P. Rebouc¸as Filho, M.B. Rodrigues, et al., Lung nodule malignancy classification in chest computed tomography images using transfer learning and convolutional neural networks, Neural Comput. Appl. 32 (2020), 11065–11082.
33. H.Y. Chiu, H.S. Chao and Y.M. Chen, Application of artificial intelligence in lung cancer, Cancers 14(6) (2022), 1370.
34. S. Mehmood, T.M. Ghazal, M.A. Khan, et al., Malignancy detection in lung and colon histopathology images using transfer learning with class selective image processing, IEEE Access 10 (2022), 25657–25668.
35. N. Kumar, M. Sharma, V.P. Singh, et al., An empirical study of handcrafted and dense feature extraction techniques for lung and colon cancer classification from histopathological images, Biomedical Signal Processing and Control 75 (2022), 103596
36. S. Tomassini, N. Falcionelli, P. Sernani, et al., Lung nodule diagnosis and cancer histology classification from computed tomography data by convolutional neural networks: A survey, Computers in Biology and Medicine (2022), 105691.
37. Y. Chen, H. Yang, Z. Cheng, et al., A whole-slide image (WSI)-based immunohistochemical feature
prediction system improves the subtyping of lung cancer, Lung Cancer 165 (2022), 18–27.
38. Y. Su, D. Li, and X. Chen, “Lung Nodule Detection based on Faster R-CNN Framework,” *Comput. Methods Programs Biomed.*, vol. 200, 2021, doi: 10.1016/j.cmpb.2020.105866.
39. L. F. Talib, J. Amin, M. Sharif, and M. Raza, “Transformer-based semantic segmentation and CNN network for detection of histopathological lung cancer,” *Biomed. Signal Process. Control*, vol. 92, no. January, p. 106106, 2024, doi: 10.1016/j.bspc.2024.106106.
40. F. Mercaldo, M. G. Tibaldi, L. Lombardi, L. Brunese, A. Santone, and M. Cesarelli, “An Explainable Method for Lung Cancer Detection and Localisation from Tissue Images through Convolutional Neural
Networks,” *Electron.*, vol. 13, no. 7, 2024, doi: 10.3390/electronics13071393.

41. A. A. Borkowski, M. M. Bui, L. B. Thomas, C. P. Wilson, L. A. DeLand, and S. M. Mastorides, "Lung and Colon Cancer Histopathological Image Dataset (LC25000)," pp. 1–2, 2019, [Online]. Available: http://arxiv.org/abs/1912.12142.
42. R. Kumar, S. Srivastava, and R. Srivastava, "A fourth order PDE based fuzzy c- means approach for segmentation of microscopic biopsy images in presence of Poisson noise for cancer detection," *Comput. Methods Programs Biomed.*, vol. 146, pp. 59–68, 2017, doi: 10.1016/j.cmpb.2017.05.003.
43. P. Kumar, S. Srivastava, and R. Srivastava, "Basic understanding of medical imaging modalities," in *High-Performance Medical Image Processing*, Apple Academic Press, pp. 1–17.
44. P. C. Yadava and S. Srivastava, "Denoising of poisson-corrupted microscopic biopsy images using fourth-order partial differential equation with ant colony optimization," *Biomed. Signal Process. Control*, vol. 93, no. October 2023, p. 106207, 2024, doi: 10.1016/j.bspc.2024.106207.
45. P. Kumar, A. Kumar, S. Srivastava, and Y. Padma Sai, "A novel bi-modal extended Huber loss function based refined mask RCNN approach for automatic multi instance detection and localization of breast cancer," *Proc. Inst. Mech. Eng. Part H J. Eng. Med.*, p. 09544119221095416.
46. A. Kumar, P. Kumar, M. Mahto, and S. Srivastava, "Breast Cancer Detection and Localization Using a Novel Multi Modal Approach," *IEEE Trans. Instrum. Meas.*, vol. 74, no. Ml, pp. 1–13, 2024, doi: 10.1109/TIM.2024.3502883.
47. B.K. Natural and H.C. Thapa, Lung cancer detection using convolutional neural network on histopathological images,*International Journal of Computer Trends and Technology* 68(10) (2020), 21–24.
48. S. Mangal, A. Chaurasia and A. Khajanchi, Convolution neural networks for diagnosing colon and lung cancer histopathological images. arXiv preprint, 2020, arXiv:2009.03878.
49. Y. Shi, Y. Gao, Y. Yang, et al., Multimodal sparse representation-based classification for lung needle biopsy images,*IEEE Trans. Biomed. Eng.* 60 (2013), 2675–2685.
50. Sethy PK, Geetha Devi A, Padhan B, Behera SK, Sreedhar S, Das K. Lung cancer histopathological image classification using wavelets and AlexNet. Journal of X-Ray Science and Technology. 2023 Jan 27;31(1):211-21.
51. Kumar A, Mehta R, Reddy BR, Singh KK. Vision transformer based effective model for early detection and classification of Lung Cancer. SN Computer Science. 2024 Aug 29;5(7):839.

AES
ISSN: 2096-3246
Volume 58, Issue 01, 2026